



## Borehole image analyses at presalt carbonate reservoirs of the Mero Field, Santos Basin

Tuany Younis Abdul Fatah, Wagner Moreira Lupinacci, Antonio Fernando Menezes Freire, Luiz Antonio Pierantoni Gamboa  
Universidade Federal Fluminense – UFF

Copyright 2019, SBGf - Sociedade Brasileira de Geofísica

This paper was prepared for presentation during the 16<sup>th</sup> International Congress of the Brazilian Geophysical Society held in Rio de Janeiro, Brazil, 19-22 August 2019.

Contents of this paper were reviewed by the Technical Committee of the 16<sup>th</sup> International Congress of the Brazilian Geophysical Society and do not necessarily represent any position of the SBGf, its officers or members. Electronic reproduction or storage of any part of this paper for commercial purposes without the written consent of the Brazilian Geophysical Society is prohibited.

### Abstract

The Mero Field was discovered in October 2010 and is currently an oil producer, having an area of 316 km<sup>2</sup>. The high quality and high productivity carbonate reservoirs in this field are characterized by microbial carbonates of the Barra Velha Formation (Aptian) and coquinas of the Itapema Formation (Barremian). The focus of this study is the facies evaluation and classification of the carbonates of the Barra Velha Formation using borehole images. Those images were integrated with the sidewall core information and helped in the understanding of four different facies (stromatolites, spherulites, grainstones and laminates), based on their textures, structures and how they interact with each other. The integration between borehole images, conventional logs, litho-geochemical logs and magnetic resonance log contributed for a better understanding and classification of facies.

### Introduction

The exploratory and production activities in presalt of the Santos Basin has brought great technological and scientific challenges due to the distance to the coast of these fields, their ultra-deep waters location, the existence of thick salt layer above the reservoirs and to a great heterogeneity of carbonate reservoirs (Karner and Gamboa, 2007; Jesus et al., 2019).

The stratigraphic characteristics of the sedimentary section and the structural complexity affect the visualization and characterization of the pre-salt reservoirs, due to the great depths of targets present mainly in the Barra Velha Formation.

The Barra Velha Formation represents the main reservoir of the presalt in the Santos Basin. This formation is believed to be deposited in a shallow and highly alkaline lacustrine environment (Szatmari & Milani, 2016). It is composed by microbial limestones, grainstones and packstones and laminites in the proximal portions, whereas in the distal portions it is composed of shales (Moreira et al., 2007). The facies found in this formation are very heterogeneous with high diagenesis and difficult to characterize.

New techniques of formation evaluation look for more accurate ways to characterize reservoirs, relating the acoustic and resistive properties of the formations with the facies types. Thus, establishing correlations with the permeable and mechanical characteristics of reservoirs (Boyd et al., 2015).

The aim of this research is the facies evaluation and classification of the presalt carbonates using borehole images acquired in Well 3-BRSA-1339A-RJS, located in Mero Field, Santos Basin. The use of borehole image is determinant when trying to establish different kinds of facies based on their textures, structures and lithology interactions. Therefore, the resistivity and acoustic images were used here to provide a better understanding of the depositional environment.

Borehole images provide high vertical and azimuthal resolution data of all logging services. They help to reduce uncertainties when integrated with other logs. These images provide accurate geological and petrophysical information which aren't easily acquired using other methods. These images lose in resolution only for conventional cores and tomography (Muniz & Bosence, 2015).

The borehole images help to understand the interactions between different lithologies and their respective internal structure, such as: bioturbation, ripple marks, beddings, erosive surfaces, unconformities, discordances and small-scale fractures and faults. It's also possible to measure the direction of those structures, adding more value to interpretation. The sidewall cores are visible in acoustic images and collaborated for a better correlation between the facies and the log images.

### Methodology

The proposed workflow is developed from the integration between borehole images, acoustic and resistivity, with sidewall cores, building a faciological model for the occurring rocks from Barra Velha Formation.

- **Image Processing**

It is performed a quality control and an image processing to correct artifacts related to logging speed, cable tension, decentralized tool, dead button or faulty pad and other related issues to improve and extract as much information possible.

After performing the quality control of the image data, another quality control is performed regarding the orientation data. All angles and directions measured during

the interpretation relies on the confiability of this orientation. The magnetometers and accelerometers data are verified and plotted along with field intensity, inclination and declination of the local magnetic field to ensure the reliability. Afterall, the magnetic declination is applied to the azimuth data.

With the corrected orientation, the resistivity images are processed. The resistivity image consists in 4 pad images separated (OBMI tool has 4 pads) and therefore they are processed as individual images to be concatenated after all the corrections.

The first and most important correction is the speed correction, which removes artifacts related to the logging speed and cable tension. Those artifacts are largely known as stick and pull (references).

Following this step, new images are generated for each pad, and these new images are then analyzed for eventual button issues, as dead buttons. When problems are found, an interpolation method is applied, if not the processing goes on.

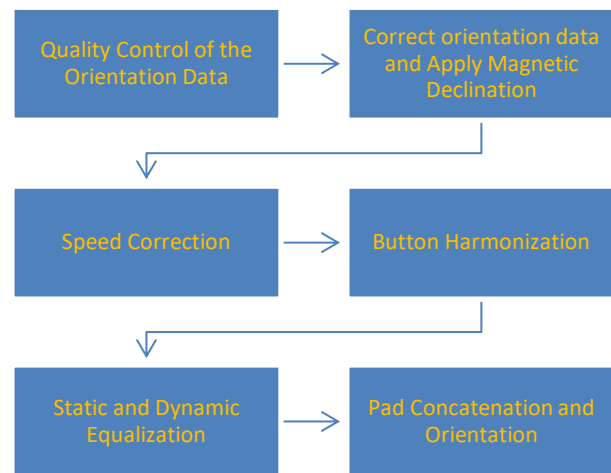
The next processing step is a button harmonization, in which a filter is applied to smooth the readings of each pad.

With all the corrections made is performed the static and dynamic equalizations. In the static equalization, the absolute values are applied to the entire image, and with this it makes possible observe unconformities, discordances and lithological boundaries. The dynamic equalization is constructed using different values to each depth interval according to a histogram evaluation. This image is used to evaluate intern structures as tiny lithological variations.

Finally, the image of each pad is concatenated and orientated according to the pad 1 azimuth, hole deviation, hole azimuth and calipers, generating a 360 degrees image, making the correct interpretation possible. The workflow applied to the resistivity image processing is shown in Figure 1.

In the present study was used two types for acoustic images: the amplitude and the travel time. They were processed following the steps described below.

The quality control of the acoustic images was performed together with the resistivity image. The correct procedure for processing the acoustic images is repeating the quality control and repair of the orientation data, applying the magnetic declination to the azimuth curves, since each tool has a different set of orientation curves.



**Figure 1: Resistivity Image processing workflow applied in Well 3-BRSA-1339A-RJS.**

The speed correction is applied but there only will be difference in the parameters applied if the tools did not log together (or in the same run).

After the speed correction, the images are oriented as the first reading of the line (or pad 1 azimuth curve), hole deviation, hole azimuth and calipers. These images are equalized generating static and dynamic images.

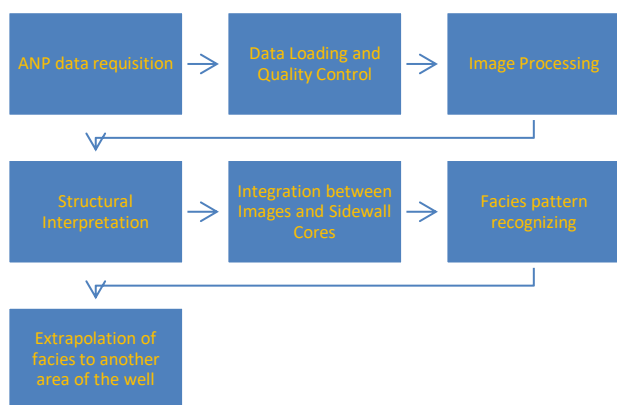
- **Image Interpretation**

An interpretation of the processed images was performed, measuring directions and dip angles of beddings, lithological contacts, fractures, faults and breakouts.

The image logs were integrated with the sidewall cores descriptions. The acoustic images were used for a better positioning of the sidewall cores, once the holes are easily observed in this image. This integration allowed the construction of a faciological model. It consists in a correlation between the observed facies found on the sidewall cores and its correspondent in the image logs. The workflow applied to the construction of the facies model and zonation in the Barra Velha Fm. in the well 3-BRSA-1339A-RJS is shown in Figure 2.

We tried to perform integration between sidewall core data and the lithologic log (present in the composite log). However, the described lithologies did not agreed. Then, we decided not to use the information contained in the lithologic log.

It is necessary to integrate the image logs with the conventional, lithogeochemical and magnetic resonance logs to extrapolate the facies model to other areas of the well, since there are not enough sidewall cores across the whole interval.



**Figure 2:** Workflow used in the construction of the facies model and zonation in the Barra Velha Fm. in the well 3-BRSA-1339A-RJS.

### Results and Discussion

The well 3-BRSA-1339A-RJS is located in Mero Field, NW of Libra's Field, Santos Basin. This well was chosen because it has a high density of quality data, providing more confidence in the performed analysis and interpretations.

Four facies were identified when the image data was integrated with the sidewall core information. These facies were classified based on the work of Terra et al. (2010), representing stromatolites, spherulites, grainstones and laminates (Figure 3). Other facies were identified; however, they are under investigation and will be "confronted with further details and information". In this work, 60 m of borehole images were interpreted and classified as the cited facies.

The stromatolite facies is represented by dendritic or arborescent textures or stromatolites heads in the amplitude acoustic image. Occasionally, it is fractured and has some vugular structures. The stromatolite facies usually occur in beds with average thickness from 2 to 3 m (Figure 4).

The spherulites were identified by spherical to subspherical texture which is associated with many fractures and vugs. The spherulites facies could be only recognized in the amplitude acoustic image. Their fractures and vugs could be also observed in the travel time image. We noted that the spherulites are usually associated with the increase of magnesium (Mg) content and the decrease of silicon (Si) content. It occurs in beds from 0.5 m to 2 m, which appears intercalated with stromatolites in some intervals. This interaction is still in analysis (Figure 4).

The grainstones facies have a massive structure in most of the observed intervals in the amplitude acoustic image, and dispersed fragments of another lithology can be also observed. In the grainstones facies, the fractures are more open, and many breakouts were observed. It was observed these fractures and breakout openings are controlled by the chemical composition with the rheology. These grainstones occurs in beds of average thickness of 2 m.

The laminates were easily recognized due to strong parallel laminations that can be observed in both images, resistivity and amplitude acoustic image logs. These facies appear in beds with average thickness of 1 m.

### Conclusions

The borehole images provided a high azimuthal resolution image, however, were not enough to characterize the entire interval. It was necessary the use of sidewall cores to determine precisely the lithology. That is why the integration of all available data is necessary to create a more reliable facies model. The integration of the borehole images, sidewall core information, conventional logs, lithochemical and magnetic resonance logs is the key to understand the depositional dynamic of the Barra Velha Formation. Four main sedimentary facies are clearly observed. The grainstone facies responds to the regional stress by fracturing whereas fracturing in the laminates is incipient. The lower part of the Barra Velha Fm is more homogenous than its upper parts where intense dips and fractures can be observed.

### Acknowledgments

The authors thank the Agência Nacional do Petróleo, Gás Natural e Biocombustíveis (ANP) for providing the data used in this research and Schlumberger for providing Techlog Software. The first author thanks CAPES for her master's scholarship and the Universidade Federal Fluminense (UFF) and the Dinâmica dos Oceanos e da Terra (DOT) Program for the provided facilities to perform this work.

### References


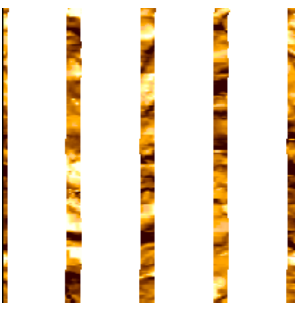
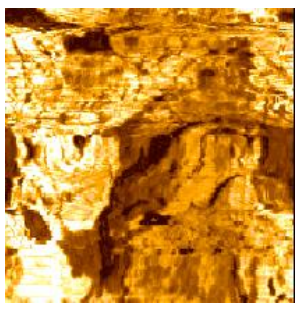



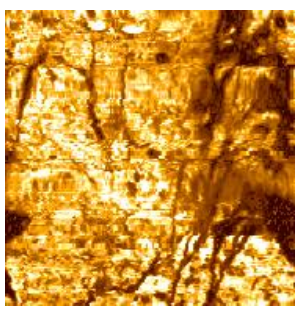


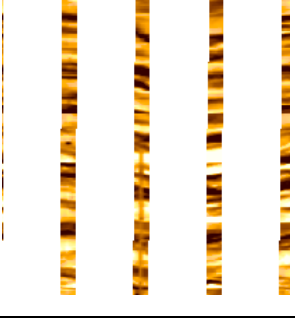
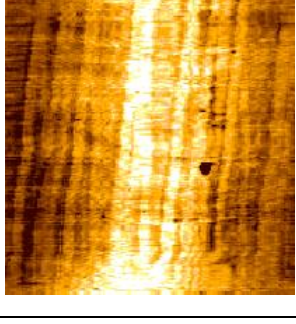


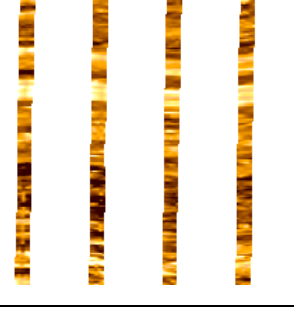
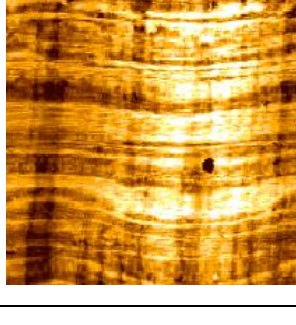

- Boyd, A., Souza, A., Giovanna, C., Machado, V., Trevizan, W., Santos, B., Netto, P., Bagueira, R., Polinski, R., and Bertolini, A. Presalt Carbonate Evaluation for Santos Basin, Offshore Brazil. *Petrophysics*: v. 56, no. 6, p. 577-597, 2015.
- Jesus, C., Olho Azul, M., Lupinacci, W.M., Machado, L. Multi-attribute framework analysis for the identification of carbonate mounds in the Brazilian Pre-Salt zone. *Interpretation*: v. 7, no. 2, p. 1-10, 2019.
- Karner, G. D., and Gamboa, L. A. P. Timing and origin of the South Atlantic pre-salt sag basins and their capping evaporites. *Geological Society London Special Publications*: v. 285, no. 1, p.15-35, 2007.
- Moreira, J. L. P., Madeira, C. V., Gil, J. A., Machado, M. A. P. Bacia de Santos. *Boletim de Geociências da Petrobras* no. 15, p. 531-549, 2007.
- Muniz, M. C., Bosence, D. W. J. Pre-salt microbialites from the Campos Basin (offshore Brazil): image log facies, facies model and cyclicity in lacustrine carbonates. In: D. W. J. Bosence, K. A. Gibbons, D. P. Le Heron, W. A. Morgan, T. Pritchard, B. A. Vining (Eds.), *Microbial Carbonates in Space and Time: Implications for Global Exploration and Production* (418). Londres: Geological Society, Special Publications, 2015.

Petersohn, E; Ferreira, M. A. Libra - Avaliação Geológica. Agência Nacional do Petróleo, Gás Natural e Biocombustíveis, 2013.

Szatmari, P. and Milani E. S. Tectonic control of the oil-rich large igneous-carbonate-salt province of the South Atlantic rift. *Marine and Petroleum Geology* no. 77, p. 567-596, 2016.

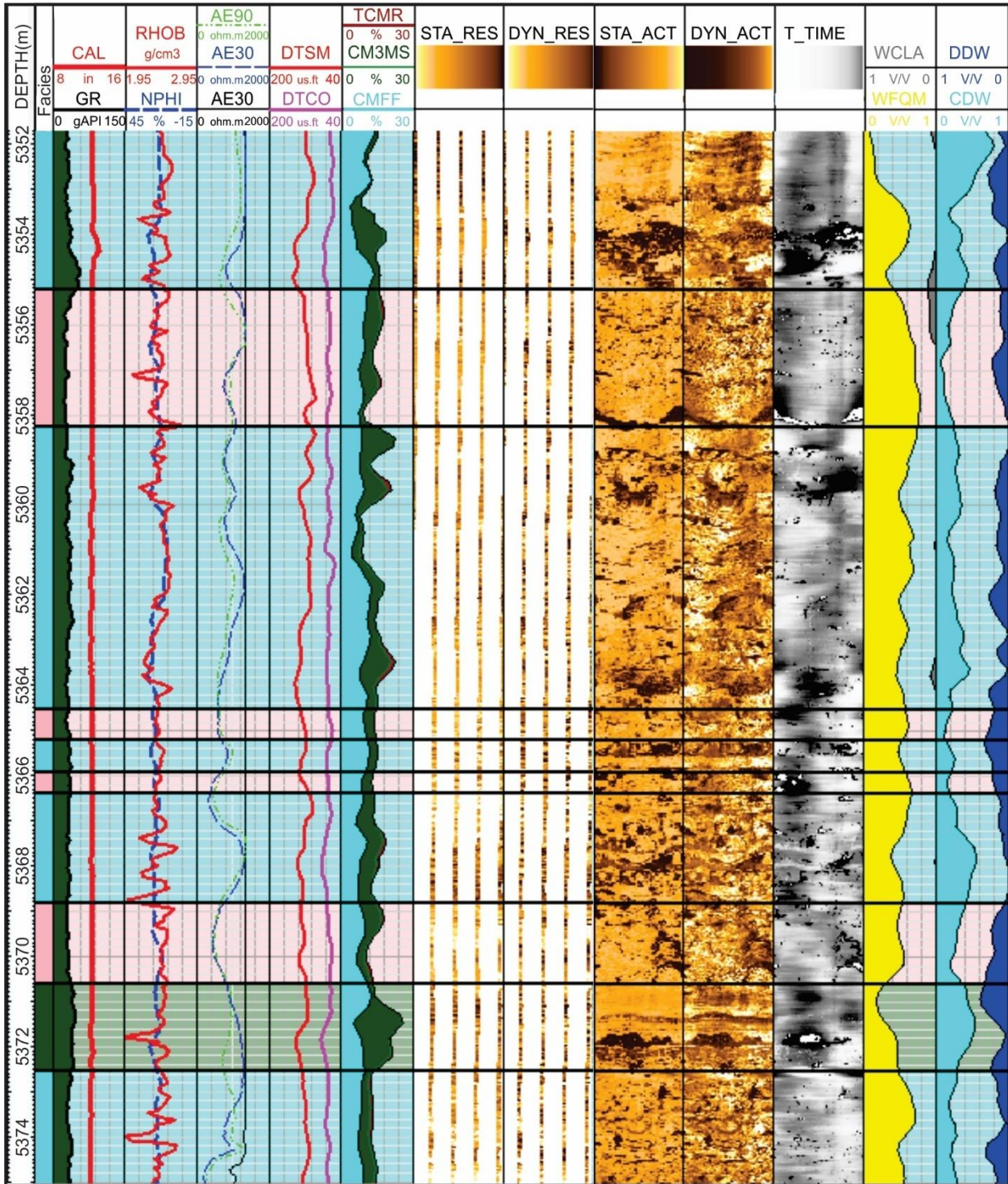
Terra, G. J. S., Spadini, A. R., França, A. B., Sombra, C., Zambonato, E., Juschaks, L. C. S., et al. Classificação de rochas carbonáticas aplicáveis as bacias sedimentares brasileiras. *Boletim de Geociências da Petrobras*, Rio de Janeiro, v.18, no.1, p. 9-29, 2010.

<http://www.ib.usp.br/evosite/evo101/IIE2aOriginoflife.shtml>  
l (26.02.2019)

Lithology	Borehole Image features	Scale	Resistivity Image Dynamic	Amplitude Acoustic Image Dynamic	Field Correlation
Stromatolite	<ul style="list-style-type: none"> <li>• Arborescent stromatolites</li> <li>• Stromatolite heads</li> </ul>				
Spherulite	<ul style="list-style-type: none"> <li>• Spherical form to subspherical</li> <li>• Highly fractured</li> <li>• Breackouts</li> <li>• Vuggy structure</li> </ul>				
Grainstone	<ul style="list-style-type: none"> <li>• Massive bedding in the Acoustic Image</li> <li>• No laminations observed in the acoustic images.</li> <li>• It is possible to observe fragments of rocks</li> </ul>				
Laminite	<ul style="list-style-type: none"> <li>• Strong laminations</li> </ul>				

**Figure 3:** Table shows the 4 (four) facies recognized in the images and their analogs in the well 3-BRSA-1339A-RJS at Barra Velha Formation. A) Estromatolites (font:www.ib.usp.br/evosite/evo101/IIIE2aOriginoflife.shtml); B) Spherulite; C) Grainstone;D) Laminite(B, C and D font: Petersohn et al. 2013).





**Figure 4:** Well 3-BRSA-1339A-RJS. Tracks: 1) Depth; 2) Zonation; 3) gamma-ray (GR) and caliper (CAL); 4) density (RHOB), neutron (NPHI) 5) resistivity (AE10, AE30, AE90); 6) sonic transit time (DTCO) and shear transit time (DTSM); 7) NMR logs: free fluid (CMFF), effective porosity (CM3MS) and total porosity (TCMR); 8) Static Resistivity Image (STA\_RES); 9) Dynamic Resistivity Image (DYN\_RES); 10) Static Amplitude Acoustic Image (STA\_ACT); 11) Dynamic Amplitude Acoustic Image (DYN\_ACT); 12) Travel Time Image (T\_TIME); 13) Dry Weight Quartz + Feldspar + Mica (WFQM) and Clay Dry Weight (WCLA); and 14) Calcite Dry Weight (CDW) and Dolomite Dry Weight (DDW). The zones delimited represent: stromatolites (blue color), spherulites (pink color), and facies still being interpreted (green color).